藏东南地区汛前洪水孕灾环境实测数据集汇编与分析

普昊琛[1,2,3]，陈　波[1,2,3*]，肖　瑶[1,2,3]，刘连友[1,2,3]，史培军[1,2,3]，
严　平[1,2,3]，张国明[1,2,3]，刘吉夫[1,2,3]

1. 北京师范大学地表过程与资源生态国家重点实验室，北京 100875；
2. 北京师范大学环境演变与自然灾害教育部重点实验室，北京 100875；
3. 北京师范大学地理科学学部，北京 100875

摘　要：气候变化背景下青藏高原受洪灾威胁逐渐增大，其东南地区河流密布且社会经济相对较为发达，因此有必要对藏东南进行洪水孕灾环境勘测。于 2021 年 6 月中下旬（汛前），采用 RD-60 手持式雷达流速仪与户外测距仪在西藏东南部 85 条河流（包括支流）进行巡测，得到藏东南地区汛前洪水孕灾环境实测 141 个点的数据集。进一步分析了藏东南地区河流流速与 Strahler 级数的关系，研究了普曲、桑曲与冷曲三条河流从河口向河源方向沿程的流速变化规律。结果表明藏东南地区汛前：（1）河流的流速普遍较大；（2）河流的平均流速随河流的 Strahler 级数增大呈指数增加；（3）同一河流的流速溯源减小，主要由径流量的减小引起。数据集内容包括：（1）藏东南 141 个测量点处河流的流速、宽度、比降、Strahler 级数与洪泛平原宽度；（2）普曲、桑曲、冷曲测量点与其河口距离。数据集存储为.shp 和.xlsx 格式，由 8 个数据文件组成，数据量为 159 KB（压缩为 1 个数据文件，37.3 KB）。

关键词：青藏高原；流速；洪水；孕灾环境
DOI: https://doi.org/10.3974/geodp.2022.01.13
CSTR: https://cstr.escience.org.cn/CSTR:20146.14.2022.01.13
数据可用性声明：
本文关联实体数据集已在《全球变化数据仓储电子杂志（中英文）》出版，可获取：
https://doi.org/10.3974/geodb.2021.10.03.V1 或 https://cstr.escience.org.cn/CSTR:20146.11.2021.10.03.V1.

1　前言

青藏高原孕育了长江、黄河、雅鲁藏布江、恒河、湄公河等多条亚洲的大江大河，在亚洲生态环境格局中具有举足轻重的特殊地位[1]。青藏高原地势呈现西北高、东南低的特点，东南部受夏季季风影响明显，气候相比西北部更为温暖湿润[2]，极端降水事件也更多[3]。西藏东南人口与经济分布相较西北部更为密集[4]。特殊的地形、气候条件下，青藏高原，

收稿日期：2021-9-15；**修订日期**：2021-12-13；**出版日期**：2022-03-25
基金项目：中华人民共和国科学技术部（2019QZKK0906，2016YFA0602404，41501020）
*通讯作者：陈波，北京师范大学地理科学学部, bochen@bnu.edu.cn
数据引用方式：[1] 普昊琛，陈波，肖瑶等. 藏东南地区汛前洪水孕灾环境实测数据集汇编与分析[J]. 全球变化数据学报，2022，6(1): 93–100. https://doi.org/10.3974/geodp.2022.01.13. https://cstr.escience.org.cn/CSTR:20146.14.2022.01.13.
[2] 普昊琛，陈波，肖瑶等. 藏东南地区汛前洪水孕灾环境实测数据集（2021）[J/DB/OL]. 全球变化数据仓储电子杂志，2021. https://doi.org/10.3974/geodb.2021.10.03.V1. https://cstr.escience.org.cn/CSTR:20146.11.2021.10.03.V1.

特别是藏东南地区，自然灾害频发，其中洪灾因常引发滑坡、泥石流等次生灾害，对交通、人口与经济等具有高的破坏性[5]。气候变化伴随的极端降水逐渐增大的趋势[1,6,7]与社会经济发展背景下，青藏高原区域的洪水及洪水-地质灾害链风险可能随之增大[3]。因此在西藏东南地区开展洪水孕灾环境的考察对促进西藏防治洪涝及其链生灾害具有实践意义。西藏地域辽阔，人口相对稀少，河流水文站点分布较为稀疏而不均匀[8,9]，水文观测数据相对较少。本研究采用实地临时测量的方法获取洪水孕灾环境数据。鉴于青藏高原的众多道路一般沿河流阶地修筑，在中国第二次青藏高原综合科学考察中，我们对公路沿线河流进行勘测。在此基础上，本文对洪水孕灾环境数据中的流速要素进行了初步分析。

2 数据集元数据简介

《藏东南地区汛前洪水孕灾环境实测数据集(2021)》[10]的元数据信息见表1。

表1 《藏东南地区汛前洪水孕灾环境实测数据集(2021)》元数据简表

条 目	描 述
数据集名称	藏东南地区汛前洪水孕灾环境实测数据集(2021)
数据集短名	Pre-flood _SETibet_2021
作者信息	普昊琛, 北京师范大学地理科学学部, 202121051170@mail.bnu.edu.cn 陈　波, AAA-2670-2022, 北京师范大学地理科学学部, bochen@bnu.edu.cn 肖　瑶, 北京师范大学地理科学学部, 202021051173@mail.bnu.edu.cn 刘连友, 北京师范大学地理科学学部, lyliu@bnu.edu.cn 史培军, 北京师范大学地理科学学部, spj@bnu.edu.cn 严　平, 北京师范大学地理科学学部, yping@bnu.edu.cn 张国明, 北京师范大学地理科学学部, zgm@bnu.edu.cn 刘吉夫, 北京师范大学地理科学学部, liujifu@bnu.edu.cn
地理区域	青藏高原东南部
数据年代	2021年6月15–26日
数据格式	.xlsx、.shp　　数据量　159 KB（压缩前），37.3 KB（压缩后）
数据集组成	8个文件（压缩为1个文件） （1）.xlsx表格文件：Sheet-1为藏东南141个测量点处河流的流速、宽度、比降、Strahler级数与洪泛平原宽度，Sheet-2、3、4分别为普曲、桑曲、冷曲测量点与其河口距离 （2）Pre-flood _SETibet_2021shp文件夹下：藏东南141个测量点位置.shp文件
基金项目	中华人民共和国科学技术部（2019QZKK0906，2016YFA0602404）
出版与共享服务平台	全球变化科学研究数据出版系统 http://www.geodoi.ac.cn
地址	北京市朝阳区大屯路甲11号100101，中国科学院地理科学与资源研究所
数据共享政策	全球变化科学研究数据出版系统的“数据”包括元数据（中英文）、通过《全球变化数据仓储电子杂志（中英文）》发表的实体数据集和通过《全球变化数据学报（中英文）》发表的数据论文。其共享政策如下：（1）“数据”以最便利的方式通过互联网系统免费向全社会开放，用户免费浏览、免费下载；（2）最终用户使用“数据”需要按照引用格式在参考文献或适当的位置标注数据来源；（3）增值服务用户或以任何形式散发和传播（包括通过计算机服务器）“数据”的用户需要与《全球变化数据学报（中英文）》编辑部签署书面协议，获得许可；（4）摘取“数据”中的部分记录创作新数据的作者需要遵循10%引用原则，即从本数据集中摘取的数据记录少于新数据集总记录量的10%，同时需要对摘取的数据记录标注数据来源[11]
数据和论文检索系统	DOI, CSTR, Crossref, DCI, CSCD, CNKI, SciEngine, WDS/ISC, GEOSS

3　数据采集方法

3.1　采集时间

数据于 2021 年 6 月 15–26 日期间采集,属于青藏高原整体及东南地区的汛前期与洪涝灾害上升初期。如图 1 所示，从 1961–2017 年降水及 1961–2010 年洪涝灾害的多年平均情况来看（图 1a），青藏高原降水与洪涝灾害均主要集中于 6–8 月，6–8 月的降水量占全年的 58%，洪涝灾害则占 81%。从 6 月开始，降水量与洪灾次数占全年总量的百分比均有明显上升。相较 5 月，6 月降水占比上升约 8%，洪灾占比则上升 14%，仅次于 7、8 月。7 月降水量在全年中占比最大，约为五分之一，洪涝灾害次数则约占全年的 34%。

在西藏东南部，6 月份降水量占全年比例较大，河流径流量开始上升，距多年平均月径流量峰值相差 1–2 个月。以奴下（雅鲁藏布江中游干流，位于林芝市米林县派镇），拉萨（拉萨河，位于拉萨市），昌都（澜沧江上游，位于昌都市）的气象（图 1b）、水文（图 1c）数据为例，从多年平均情况来看，6 月份月径流量则占全年总量的 10%–13%，位于第 4；月降水量（1997 年）占全年总量的 17%–20%，位于第 3。除此之外，不同地区径流峰值出现时间有一定差异，奴下站与拉萨站月径流峰值出现在 7 月，昌都站则出现于 8 月。在汛期初期进行洪水孕灾环境勘测，能一定程度上刻画洪水水文特征，也能保证安全、顺利开展测量工作。

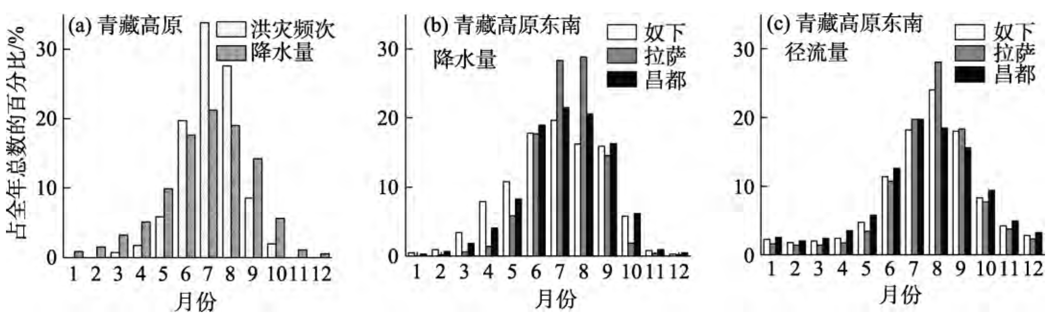

图 1　青藏高原及其东南部降水、径流特征：（a）青藏高原月降水量与洪灾频次（据马伟东，2019 改绘[12]）；（b）藏东南部分气象站月降水量占全年总数百分比（据阮本清，2000[13]改绘）；（c）藏东南部分水文站月径流量占全年总数百分比（据刘国纬，1992[14]；阮本清，2000[13]改绘）

3.2　采集方法

测量数据包括河流流速、水面宽度、洪泛平原宽度和河流比降等。流速采用 RD-60 手持式雷达流速仪（图 2a）进行测量。该仪器采用 K 波段雷达，可对河流、污水、泥浆、海洋等进行非接触式的流速测量，体积小巧、电池供电、可手持式操作、使用简便。水面宽度及洪泛平原宽度的测量仪器为两种手持户外测距仪，均利用脉冲测量距离，量程分别为 1,500 m（图 2b）和 1,000 m（图 2c），在各种光照条件下测量都能保证精度。其中，水面宽度为测量时刻所见的水面宽度，洪泛平原宽度为河流两岸临河植被带之间的宽度。测量点处的河流比降为测量点上下游各 200 m 处的高程差与流程长度（400 m）的比值，在室内基于 Google Earth 完成。

图 2　数据采集设备：（a）测量河流流速用的 RD-60 手持式电波（雷达）流速仪；（b）和（c）测量水面宽度、洪泛平原宽度的两种测距仪

流速测量主要在桥梁上完成。一是流速测量仪器推荐在桥梁上开展测量，二是青藏高原地区桥梁是相对容易接近水流的位置，便于选取合适的测量点，控制测量角度，以保证测量的可达性和精确性[15]（图 3）。测量所处的桥梁横跨大小不等的河溪，如较大的通麦特大桥（横跨帕隆藏布支流易贡藏布，全长 415.8 m），中等的帕当桥（横跨雅鲁藏布江，全长 225 m），和较小的木桥与铁桥（证该曲小桥，拉布桥，均为 2–3 m 长）等。本数据采集过程中，采用单点法在河道深泓线附近区域测量水面流速。一般河道流速测量首先在过水断面上设置 5 个或更多从河面到河底的测量垂线，并在每一垂线上采用单点、三点或五点垂线法在不同水深处测速[16]。由于青藏高原地区河流谷深水急风大，精细流速测量具有一定的危险性，加之本次河流洪水特征简要调研覆盖面广而时间安排紧凑，因此我们选择以深泓线附近水面流速作为该处河流流速。河流水面宽度、洪泛平原宽度的测量一般在桥两端或岸边最近点进行测量。为尽量控制测量误差，对于流速，水面宽度、洪泛平原宽度等数值，每个测点测量三次，取三次平均值为最终值。

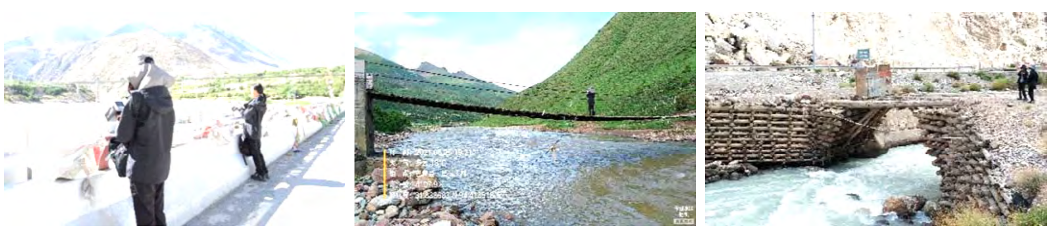

图 3　在横跨大小不等的河流的桥上测量流速

3.3　覆盖范围

于 141 个流速测量点采集的数据覆盖 85 条河，遍布 23 个县区，沿河里程 2,000 余 km（图 4）。所测量河流中，大河（Strahler 河流分级[17]5 级以上）有 41 个测量点，包括西藏地区主要河流雅鲁藏布江、怒江、澜沧江、尼洋河等，共 19 条；中等河流（3–5 级）有 80 个测量点，包括更张曲、米堆曲、普曲、冷曲等 45 条河流；小河流（1–2 级）共 20 个测量点，包括滨达曲、打曲等约 10 条河流。除大范围进行流动测量外，我们还对部分具有不同规模流域进行细致的洪水孕灾环境查勘，其中包括普曲（图 4a）、冷曲（图 4b）、桑曲（图 4c）等，以及扎曲、郎学杰沟、米堆曲等的细致查勘，限于篇幅，此处不作详细说明。从测量点流速的整体空间分布可见，越靠近南部，高流速出现的频次越多；从单条河流来看，由上游山区到下游河口，流速呈逐渐增大趋势；较大流速多出现于河流交汇处。

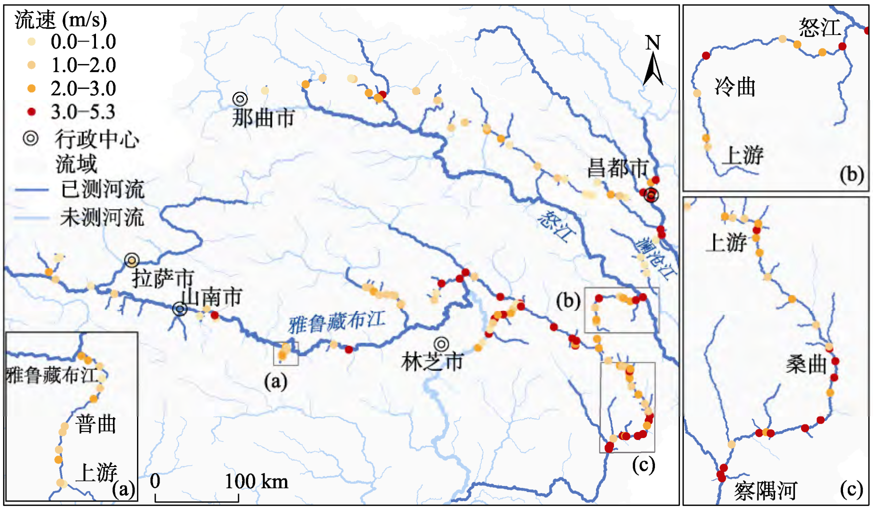

图 4　流速测量点分布图

4　数据结果

基于本次科考采集的数据，初步分析了青藏高原东南部河流流速特征，包括流速与河流级数的关系及流速从河口到河源的沿程变化规律。

4.1　数据集分布

藏东南作为径流高值区域[18]，其流速与比降均较大。图 5 显示了 2021 年 6 月 15–26 日藏东南地区河流流速与比降的统计分布。由图 5a 可见，在 141 个测量点中，2 m/s 以上的测点有 70 个，约占 50%；其中位于(1.25，1.5]速度区间的测点数最多，为 15 个，占 10.6%。流速超过 4 m/s 以上的测点有 11 个，主要位于测点分布范围中的东南部分（图 4），其中三个来自察隅河东支桑曲，两个来自于米堆冰川米堆曲，两个来自于额公藏布波密段附近。本次测得的最大流速为 5.32 m/s，位于林芝市波密县扎木镇达兴村额公藏布达兴中桥下。如图 5b 所示，藏东南地区河流比降普遍较大，呈指数分布。约 80%测量河段的测点比降大于 10‰，超过 50%的测量河段处比降大于 2%。其中河段比降大于 30%的有 3 个测量点，分别是为 48%，35%和 32%。其中最大的两个位于扎墨公路途经嘎弄曲支流处，最后一个位于昌都市八宿县果洛村附近惹那通曲处。这三个测量点均位于由陡峭山坡以接近垂直河谷的角度汇入河谷的河流。藏东南地区水急坡陡，在经过强降水后洪水的汇流时间较短，因此常形成发生时间短、强度大的山洪，造成较大的经济损失与人、畜伤亡[19]。

4.2　流速与河流级数的关系

从采集的数据来看，青藏高原东南部河流的流速与 Strahler 河流级数呈指数函数关系（图 6）。按照传统的 Strahler 河流特征分析方法[20]，图 6 展示了按照河流级数分类统计的测量情况及河流流速特征值。尽管同一级数河流的流速具有较大的变化，但总体来讲，河流平均流速（v）随着 Strahler 河流级数（ω）的增大呈指数增加，拟合所得指数函数为：

$$v = 1.116e^{0.158(\omega-1)} \tag{1}$$

在 p<0.001 的显著性水平下，河流级数解释了河流平均流速方差的 91%（R^2 = 0.911）。青

藏高原东南部实测 1 级河流的平均流速为 1.10 m/s，根据式(1)的拟合值则为 1.12 m/s。尽管该河流流速-级数关系有一定的拟合误差，但可用于青藏高原东南资料稀缺地区的流速简易推算。

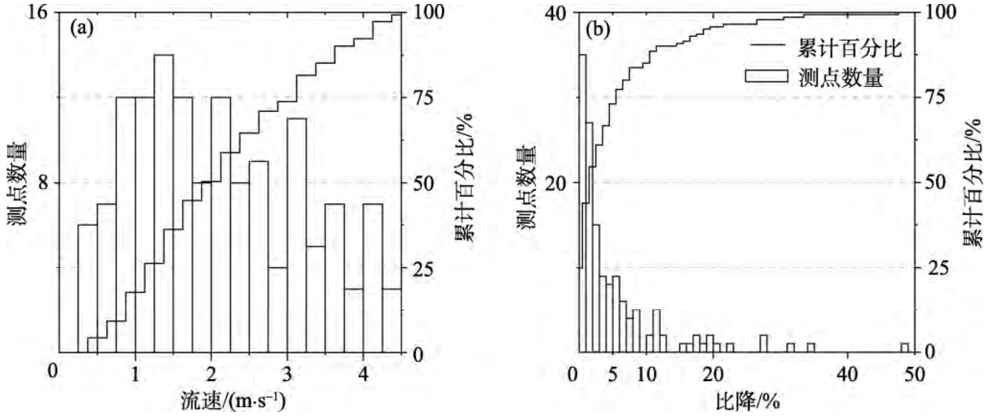

图 5 测量点流速统计分布（a）与比降统计分布（b）

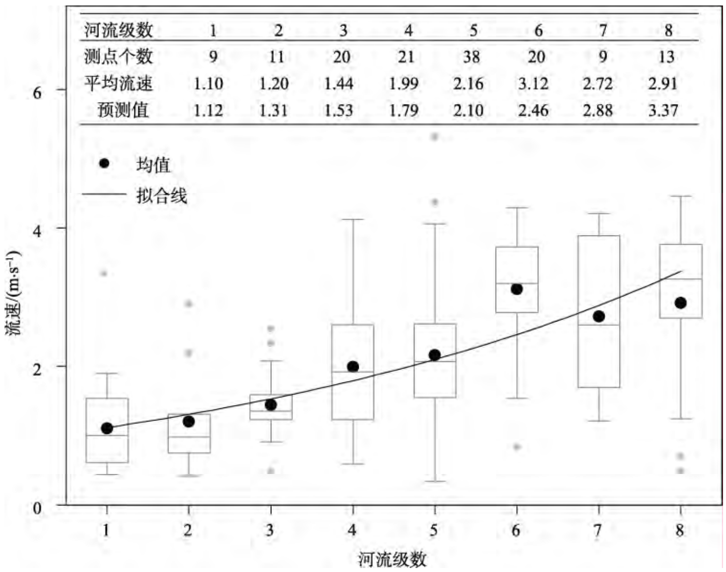

河流级数	1	2	3	4	5	6	7	8
测点个数	9	11	20	21	38	20	9	13
平均流速	1.10	1.20	1.44	1.99	2.16	3.12	2.72	2.91
预测值	1.12	1.31	1.53	1.79	2.10	2.46	2.88	3.37

图 6 藏东南地区河流流速与河流级数之间的关系

4.3 流速从河口到河源的沿程变化规律

以青藏高原东南部三条不同 Strahler 级数的河流桑曲、冷曲与普曲为例，探索了流速由河口溯源而上的沿程变化规律。桑曲为东支察隅河主流，位于林芝市察隅县，为 6 级河。沿该河干流布设 14 个测量点，测量里程约 150 km，测量河段有 4 条 5 级河流汇入。冷曲为怒江支流，位于昌都市八宿县，为 5 级河，其支流包括瓦曲。沿该河干流共有 9 个测量点，测量长度约 100 km，测量河段有 5 条 4 级河流汇入。普曲为雅江支流，位于山南市朗县，为 5 级河。沿该河干流共有 11 个测量点，测量里程约 15 km。

由河口溯源而上，流速沿程大体逐渐减小。图 7 展示桑曲、冷曲和普曲三条河流流速、水面宽度和比降由河口向河源方向沿程变化情况。从流速与距河口流程长度的简单线性拟

合来看：斜率均为负值，依次为是–0.009，–0.017，–0.044（不含奇异值）；拟合关系显著性水平依次为<0.01，<0.01 和<0.1（不含奇异值）。可见三条河流的流速溯源减小。这与“山区河流比降相对较大，因此其流速可能大于下游相对平缓河段”结论有出入。

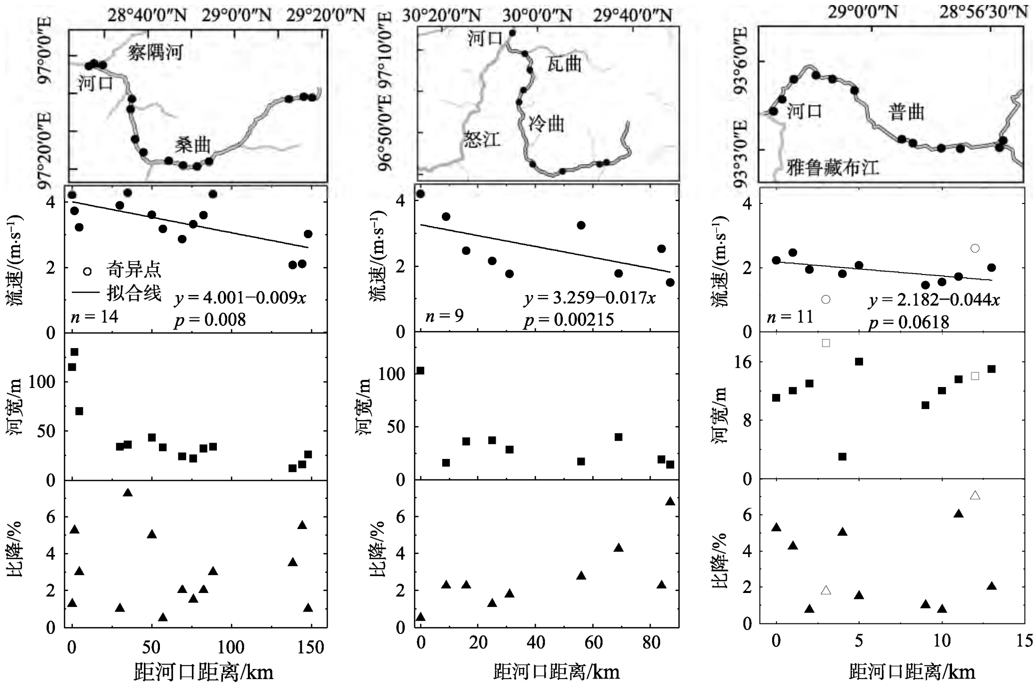

图 7　桑曲、冷曲与普曲从河口向河源方向沿程河流的流速、河宽和比降变化

由曼宁方程可知，河流比降和水力半径（在河宽远大于水深的情况下，水力半径近似等于水深）都是河流流速的主要影响因素[21]。上游河段一般比降较大，但下游随着汇水面积或汇流支流个数的增加而径流量（或水深）增大，因此，沿同一河流从源区向河口方向的流速变化由比降与水量竞争决定。上述数据及分析表明，本次测量的青藏高原东南区的桑曲、冷曲与普曲三条河流，越靠近河口，汇水面积越大或汇入支流越多，水量增大所带来的流速增加效应在一定程度上超过了比降减小所带来的流速降低效应。尽管河流流速从河口溯源沿程大致减小，但整体趋势可能因局地的比降和河宽变化而呈现小的波动。如普曲在测量河宽最大值处与比降最大值处（图 7 中的空心符号），显示出与整体趋势相异的流速。包含这两处测量值奇异点时，所得的普曲拟合方程斜率为–0.004 且统计检验为不显著；不包含它们时，流速溯源下降趋势变为每公里 0.044m/s，且通过 p=0.1 的水平上的统计显著性检验。这表明，由于普曲两侧汇入支流较少，河流水量增加不如桑曲、冷曲明显，流速虽然随河口溯源而上有下降的趋势，但更容易受局地河段比降及河宽的影响。因此去除奇异点之后，其流速随距河口里程的变化关系可能更符合真实情况。

5　讨论和总结

本数据集基于 RD-60 手持式电波（雷达）流速仪与手持户外测距仪，通过实地测量所得。通过分析数据的统计分布特征、流速与河流级数的关系及流速从河口溯源的沿程变化

规律，得到以下结论：相较平原，青藏高原河流流速普遍偏大；流速总体表现为河流级别越大，流速越快；在青藏高原部分河流，体现出距离河口越近的位置河流流速越快，河流流速的增加主要来源于径流量的增加。本文对于流速数据的采集和分析，可以为藏东南资料稀缺地区的流速估算提供依据，并阐明该地区河流流速变化的主要影响因素，从而可以更好的掌握藏东南地区洪水汇流特点，为该地区的洪水灾害模拟及风险防范提供参考。

作者分工：陈波、普昊琛、肖瑶对数据集的开发做了总体设计；肖瑶、普昊琛、陈波采集、处理和分析了数据；普昊琛、陈波撰写了数据论文；刘连友、史培军、严平、张国明、刘吉夫等教授指导了数据的采集方案，修订了论文稿件。

致谢：感谢与杨文涛副教授的有益讨论，感谢欧珠培杰师傅等在数据采集过程中提供耐心而细致的帮助。

利益冲突声明：本研究不存在研究者以及与公开研究成果有关的利益冲突。

参考文献

[1] 傅敏宁. 青藏高原气候变化响应对我国防灾减灾的挑战[J]. 中国减灾, 2021(7): 46–49.
[2] 王晓军, 程绍敏. 西藏主要气候特征分析[J]. 高原山地气象研究, 2009, 29(4): 81–84.
[3] 马伟东, 刘峰贵, 周强等. 1961–2017 年青藏高原极端降水特征分析[J].自然资源学报, 2020, 35(12): 3039–3050.
[4] 戚伟, 刘盛和, 周亮. 青藏高原人口地域分异规律及"胡焕庸线"思想应用[J]. 地理学报, 2020, 75(2): 255–267.
[5] 吴积善, 程尊兰, 耿学勇. 西藏东南部泥石流堵塞坝的形成机理[J]. 山地学报, 2005(4): 4399–4405.
[6] 李林, 陈晓光, 王振宇等. 青藏高原区域气候变化及其差异性研究[J]. 气候变化研究进展, 2010, 6(3): 181–186.
[7] 徐丽娇, 胡泽勇, 赵亚楠等. 1961–2010 年青藏高原气候变化特征分析[J]. 高原气象, 2019, 38(5): 911–919.
[8] 巩同梁, 王秀娟, 谢玉红等. 西藏水文监测网络空间分布特征[J]. 水文, 2004(6): 41–43.
[9] Lan, C., Zhang, Y. X., Zhu, F. X., *et al*. Characteristics and changes of streamflow on the Tibetan Plateau: a review [J]. *Journal of Hydrology*: *Regional Studies*, 2014, 2: 49–68.
[10] 普昊琛, 陈波, 肖瑶等. 藏东南地区汛前洪水孕灾环境实测数据集(2021)[J/DB/OL]. 全球变化数据仓储电子杂志, 2021. https://doi.org/10.3974/geodb.2021.10.03.V1. https://cstr.escience.org.cn/CSTR:20146.11.2021.10.03.V1.
[11] 全球变化科学研究数据出版系统. 全球变化科学研究数据共享政策[OL]. https://doi.org/10.3974/dp.policy.2014.05(2017 年更新).
[12] 马伟东. 青藏高原极端降水特征及洪涝灾害临界雨量估算[D]. 西宁: 青海师范大学, 2019: 58.
[13] 阮本清, 王浩. 西线调水区水资源分析及可调水量商榷[J]. 清华大学学报(自然科学版), 2000(S1): 101–106.
[14] 刘国纬. 西藏高原的水文特征[J]. 水利学报, 1992(5): 1–8.
[15] 宗先国, 王健, 许文阁. 桥测技术在鲁北平原区巡测中的应用[J]. 水文, 2004, 24(3): 46–50.
[16] 左建, 邓山, 张洪霞等. 白河水文站表面流速代表性研究[J]. 水文, 2021, 41(3): 19–24.
[17] Strahler, A. N. Quantitative analysis of watershed geomorphology [J]. *Eos, Transactions American Geophysical Union*, 1957, 38(6): 913–920.
[18] 张丁玲. 青藏高原水资源时空变化特征的研究[D]. 兰州: 兰州大学, 2013: 165.
[19] 高懋芳, 邱建军. 青藏高原主要自然灾害特点及分布规律研究[J]. 干旱区资源与环境, 2011, 25(8): 101–106.
[20] Downing, J. A., Cole, J. J., Duarte, C. M., *et al*. Global abundance and size distribution of streams and rivers [J]. *Inland Waters*, 2012, 2(4): 229–236.
[21] Jain, S. C. Open-channel Flow [M]. Hoboken: John Wiley & Sons, 2000.

Journal of Global Change Data & Discovery. 2022, 6(1): 93-100
www.geodoi.ac.cn

Global Change Research Data Publishing & Repository

Characteristics of Pre-flood Season Flow Velocity in Southeastern Tibet, China

Pu, H. C.[1,2,3] Chen, B.[1,2,3*] Xiao, Y.[1,2,3] Liu, L. Y.[1,2,3] Shi, P. J.[1,2,3] Yan, P.[1,2,3] Zhang, G.M.[1,2,3] Liu, J. F.[1,2,3]

1. The State Key Laboratory of Earth Surface Processes and Resource Ecology, Beijing Normal University, Beijing 100875, China;
2. The Key Laboratory of Environmental Change and Natural Disaster, Beijing Normal University, Beijing 100875, China;
3. Faculty of Geographical Science, Beijing Normal University, Beijing 100875, China

Abstract: The Tibetan Plateau is increasingly threatened by floods under climate change. The densely distributed rivers and relatively more developed socioeconomic conditions in southeastern Tibet make it necessary to survey flood characteristics across this region. Using a handheld radar current meter (RD-60) and outdoor rangefinders, a dataset of 141 samples from 85 rivers in southeastern Tibet was collected during a field survey from mid to late June 2021 (the pre-flood season). Based on this dataset, we investigated the relationship between stream flow velocity and Strahler stream order and the pattern of flow velocity from the river mouth to the channel head for the Sangqu, Lengqu and Puqu rivers. The results showed that during the pre-flood season in southeastern Tibet: (1) the stream flow velocity is generally higher than that measured for nonmountainous rivers; (2) the average stream flow velocity increases exponentially with Strahler stream order; and (3) the flow velocity decreases from the mouth to the head of a stream, owing to the decrease in stream discharge toward the head. The dataset includes (1) flow velocity, river width, channel slope, Strahler order and floodplain width measured at 141 locations on 85 rivers in Southeast Tibet and (2) the distances of the sampling points measured from the river mouths for the Sangqu, Lengqu and Puqu rivers. The dataset is archived in .shp and.xlsx data formats, consists of 8 data files and has a size of 159 KB (compressed into a single file of 37.3 KB).

Keywords: Tibetan Plateau; stream flow velocity; flood; floodplain characteristics

DOI: https://doi.org/10.3974/geodp.2022.01.13

CSTR: https://cstr.escience.org.cn/CSTR:20146.14.2022.01.13

Dataset Availability Statement:

The dataset supporting this paper was published and is accessible through the *Digital Journal of Global Change Data Repository* at: https://doi.org/10.3974/geodb.2021.10.03.V1 or https://cstr.escience.org.cn/CSTR:20146.11.2021.10.03.V1.

Received: 15-09-2021; **Accepted:** 13-12-2021; **Published:** 25-03-2022

Foundations: Ministry of Science and Technology of P. R. China (2019QZKK0906, 2016YFA0602404)

***Corresponding Author:** Chen, B., Faculty of Geographical Science, Beijing Normal University, bochen@bnu.edu.cn

Data Citation: [1] Pu, H. C., Chen, B., Xiao, Y., *et al*. Characteristics of preflood season flow velocity in Southeastern Tibet, China [J]. *Journal of Global Change Data* & *Discovery*, 2021, 6(1): 93–100. https://doi.org/10.3974/geodp.2022.01.13. https://cstr.escience.org.cn/CSTR:20146.14.2022.01.13.

[2] Pu, H. C., Chen, B., Xiao, Y., *et al*. Pre-flood environment field survey dataset in Southeastern Tibet of China (2021) [J/DB/OL]. *Digital Journal of Global Change Data Repository*, 2021. https://doi.org/10.3974/geodb.2021.10.03.V1. https://cstr.escience.org.cn/CSTR:20146.11.2021.10.03.V1.

1 Introduction

The Qinghai-Tibet Plateau is the origin of many major rivers in Asia such as the Yangtze river, the Yellow river, the Yaluzangbu river, the Ganges river and the Mekong river, and is crucial for the ecological security of Asia[1]. Southeast Tibet is demonstrably affected by the summer monsoon. Therefore, there are more extreme precipitation events[2], and the climate is warmer and wetter than that in the northwest[3]. The population and economy are more densely distributed in Southeast Tibet than in Northwest Tibet[4]. With the spatial configuration of terrain and climate, natural disasters occur frequently in the Qinghai-Tibet Plateau, particularly in Southeast Tibet. Floods often cause secondary disasters such as landslides and debris flows, which are highly destructive to the population, the economy, and transportation routes[5]. With the increasing trends of extreme precipitation under climate change[1,6,7] and socio-economic development, the risk of flood and flood-geological disaster cascades may increase in the Qinghai-Tibet Plateau[3]. The Qinghai-Tibet Plateau covers a vast area and has relatively sparse population, and there are relatively few hydrological data due to the sparse distribution of hydrological stations[8,9]. Therefore, conducting field surveys of flood characteristics in the Qinghai-Tibet Plateau is of practical significance to facilitate risk prevention of floods and their disaster cascades in this region.

Table 1 Metadata summary of the Pre-flood environment field survey dataset in Southeastern Tibet of China (2021)

Items	Description
Dataset full name	Pre-flood environment field survey dataset in Southeastern Tibet of China (2021)
Dataset short name	Pre-flood _SETibet_2021
Authors	Pu, H. C., Faculty of Geographical Science, Beijing Normal University, 202121051170@mail.bnu.edu.cn Chen, B., AAA-2670-2022, Faculty of Geographical Science, Beijing Normal University, bochen@bnu.edu.cn Xiao, Y., Faculty of Geographical Science, Beijing Normal University, 202021051173@mail.bnu.edu.cn Liu, L. Y., Faculty of Geographical Science, Beijing Normal University, lyliu@bnu.edu.cn Shi, P. J., Faculty of Geographical Science, Beijing Normal University, spj@bnu.edu.cn Yan, P., Faculty of Geographical Science, Beijing Normal University, yping@bnu.edu.cn Zhang, G. M., Faculty of Geographical Science, Beijing Normal University, zgm@bnu.edu.cn Liu, J. F, Faculty of Geographical Science, Beijing Normal University, liujifu@bnu.edu.cn
Geographical region	Southeastern Qinghai-Tibet Plateau
Year	June 15 to June 26, 2021 Data format .xlsx, .shp
Data size	159 KB (before compression); 37.3 KB (after compression)
Data files	8 files (compressed into 1 file) (1) .xlsx table file: sheet 1 is the stream flow velocity, river width, channel slope, Strahler order and floodplain width at 141 measuring points in southeastern Tibet. Sheets 2, 3 and 4 are the distances from the measuring point of Puqu river, Sangqu river and Lengqu river to their river mouth, respectively (2) Preflood _SETibet_2021 shp folder:.shp format file of the location of 141 measurement points in southeastern Tibet
Foundations	Ministry of Science and Technology of P. R. China (2019QZKK0906, 2016YFA0602404)
Data publisher	Global Change Research Data Publishing & Repository, http://www.geodoi.ac.cn
Address	No. 11A, Datun Road, Chaoyang District, Beijing 100101, China
Data sharing policy	***Data*** from the Global Change Research Data Publishing & Repository includes metadata, datasets (in the *Digital Journal of Global Change Data Repository*), and publications (in the *Journal of Global Change Data & Discovery*). ***Data*** sharing policy includes: (1) ***Data*** are openly available and can be free downloaded via the internet; (2) end users are encouraged to use ***Data*** subject to citation; (3) users, who are by definition also value-added service providers, are welcome to redistribute ***Data*** subject to written permission from the GcdataPR Editorial Office and the issuance of a ***Data*** redistribution license; and (4) if ***Data*** are used to compile new datasets, the 'ten percent principal' should be followed such that ***Data*** records utilized should not surpass 10% of the new dataset contents, and sources should be clearly noted in suitable places in the new dataset[11]
Communication and searchable system	DOI, CSTR, Crossref, DCI, CSCD, CNKI, SciEngine, WDS/ISC, GEOSS

2 Metadata of the Dataset

The metadata of the Pre-flood environment field survey dataset in Southeastern Tibet of China (2021)[10] is summarized in Table 1.

3 Data Acquisition Method

3.1 Acquisition Time

The data were collected from June 15 to June 26, 2021, during the early stage of the flood season for the entire Qinghai-Tibet Plateau and its southeast. Figure 1a displays the monthly distribution of long-term average precipitation (1961–2017) and flood disasters (1961–2010). Precipitation and flood disasters on the Qinghai-Tibet Plateau mainly occur during the period from June to August. The precipitation and flood disaster distribution from June to August accounts for 58% and 81% of the entire year, respectively. Compared with May, the proportion of precipitation and number of flood events in June increased by approximately 8% and 14%, respectively and were second only to levels in July and August. The precipitation in July accounts for the largest proportion of the annual total, about 20%, and the number of flood disasters accounts for approximately 34% of the total for the year.

In Southeast Tibet, in June, precipitation accounts for a large proportion of the entire year, and river runoff begins to rise, which is approximately 1–2 months prior to the time of peak monthly runoff. Using the hydrological and meteorological (Figure 1) data for Nuxia (the main channel of the middle reaches of the Yaluzangbu river, located in Pai town, Milin county, Linzhi city), Lasa (Lasa river) and Changdu (the upper reaches of the Lancang river) as examples, the monthly runoff in June accounts for 10%–13% of the total annual volume and ranks fourth for the year; monthly precipitation in June accounts for 17%–20% of the annual total precipitation and ranks third for the year. In addition, the timing of peak runoff varies across regions. The monthly peak runoffs of the Nuxia and Lasa stations occur in July, whereas that of the Changdu station occurs in August. Conducting surveys at the beginning of the flood season can not only describe the hydrological characteristics of the flood to a certain extent, but help to safely record the hydrological characteristics of floods.

3.2 Acquisition Method

Measurements were made for stream flow velocity, stream width, floodplain width and channel slope during the field survey. Flow velocity was measured using a RD-60 handheld radar flow meter (Figure 2a). The instrument uses K-band radar to measure the flow velocity of rivers, sewage and oceans without contact. It has the advantages of compact size, a battery power supply, handheld operation and being simple to use. The instruments for measuring river width and floodplain width were two types of handheld outdoor rangefinders that use pulses to measure distance and can ensure accuracy under various lighting conditions. The measuring ranges were 1,500 m (Figure 2b) and 1,000 m (Figure 2c). River width refers to the maximum width of the water at the time of measurement, and floodplain width refers to the distance between the riverside vegetation zones on both banks. The channel slope at the measurement point is the ratio of the elevation difference at 200 m upstream and downstream of the measurement point to the flow length (400 m). Channel slope measurements were completed indoors using Google Earth.

Velocity was mainly measured from bridges for two reasons: first, a velocity measuring instrument is recommended for use on bridges; second, on the Qinghai-Tibet Plateau, bridges are ideal locations to approach water flow because it is convenient to select appropriate measurement points and control the measurement angle, which ensures the accessibility and accuracy of measurement[15] (Figure 3).

The bridges selected for the survey were located on rivers of different sizes such as the

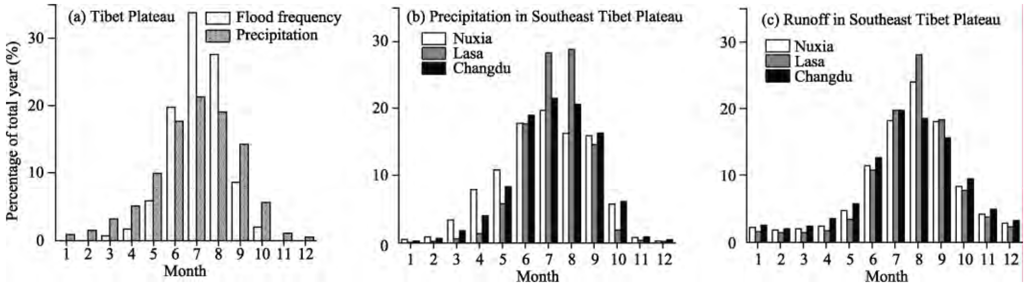

Figure 1 The precipitation and runoff characteristics of the Qinghai-Tibet Plateau and its southeastern region: (a) monthly precipitation and flood frequency on the Qinghai-Tibet Plateau (based on Ma 2019[12], modified); (b) percentage of precipitation relative to the annual total at three weather stations in southeastern Tibet (based on Ruan 2000[13], modified); and (c) percentage of runoff relative to the annual total at three hydrological stations in southeastern Tibet (based on Liu 1992[14] and Ruan 2000[13], modified)

Figure 2 Data acquisition equipment: (a) the handheld radar current meter (RD-60) for measuring stream flow velocity, and two outdoor rangefinders; (b) and (c), used to measure river width and floodplain width

Figure 3 Measuring flow velocity on rivers of various sizes

Tongmaiteda bridge (across the Yigongzangbu river, a tributary of the Palongzangbu river, with a total length of 415.8 m), the medium-sized Padang bridge (across the Yaluzangbu river, with a total length of 225 m), and the small wooden and iron bridges (such as the QuXiao bridge and Labu bridge, both of which are 2–3 m long). In the process of data acquisition, the single-point method is used to measure the velocity near the channel thalweg. In general river velocity measurement, firstly, five or more measurement vertical lines from the river surface to the river bottom are set on the wetted cross section, and then the velocity is measured at different water depths by single- point, three-point or five-point vertical line method on each vertical line[16]. Because the Qinghai-Tibet Plateau has the characteristics of a deep river valley with rapid water and strong winds, the typical flow velocity measurement approach is dangerous and often not feasible. In addition, the flood survey covered a large area and had a tight schedule. Therefore, flow velocities were measured using the single point approach at river centerlines. The widths of the rivers and floodplains were generally measured at both ends of the bridge or at the nearest bank point. To reduce measurement error, three measurements of flow velocity, river width and floodplain width were made at each sampled location, and the average was taken as the final value.

3.3 Data Coverage

The data were collected at 141 locations on 85 rivers in 23 counties over more than 2,000 km of river (Figure 4). Among the rivers surveyed there were: (1) 41 survey locations for large rivers (Strahler order[17] greater than 5), including 19 major rivers in Tibet such as the Yaluzangbujiang river, Nujiang river, Lancangjiang river, and Niyanghe river; (2) 80 survey locations for medium rivers (Strahler order 3–5), including 45 rivers such as the Gengzhangqu river, Miduiqu river, Puqu river and Lengqu river; and (3) 20 survey locations for small rivers (Strahler order 1–2), including approximately 10 rivers such as the Bindaqu river and Daqu river. In addition to flow velocity measurements, we also conducted a detailed survey for a few watersheds of various sizes, including the Puqu river (Figure 4a), Lengqu river (Figure 4b), Sangqu river (Figure 4c), Zhaqu river, Langxuejiegou river, and Miduiqu river. As shown in Figure 4, high flow velocities tended to cluster southeast of the surveyed area, and flow velocity appears to increase gradually downstream from the mountainous area.

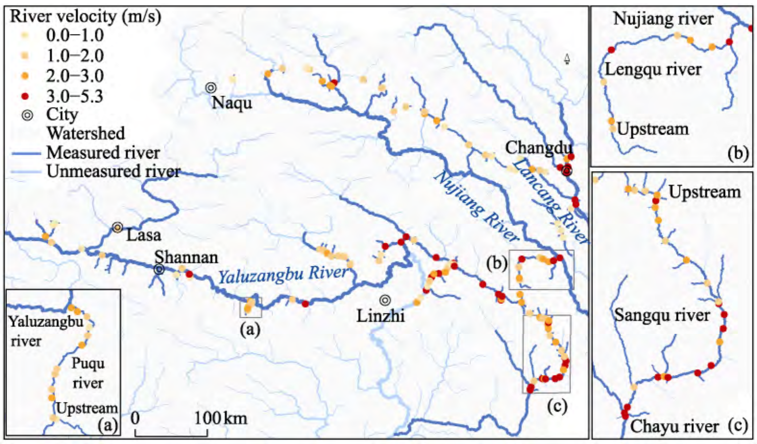

Figure 4 Distribution of survey locations

4 Data Results

Based on the data collected by the survey, flow velocity characteristics in the southeastern Qinghai-Tibet Plateau are analyzed, including the relationship between velocity and Strahler order and the pattern of velocity from the river mouth to its headwater.

4.1 Statistical Summary of Flow Velocities

The flow velocity and channel slope are relatively large in Southeast Tibet, which is a region with high discharge[18]. Figure 5 shows the statistical distribution of stream flow velocity and slope in Southeast Tibet from June 15 to June 26, 2021. As shown in Figure 5a, among the 141 measuring points, 70 measuring points have velocities above 2 m/s, accounting for approximately 50% of points; 15 measuring points (10.6%) fall within the velocity range of (1.25, 1.5]. There are 11 measuring points with velocities above 4 m/s, mainly located in the southeast of the surveyed region (Figure 4). Included in these measurements are velocities from the Sangqu river (3 measurements), the Miduiqu River in Midui glacier (2 measurements) and the Bomi county section of the Egongzangbu river (2 measurements). The maximum velocity of survey (5.32 m/s) was measured at the Daxing middle bridge over the Egongzangbu river in Daxing village of Bomi county. As shown in Figure 5b, the channel slopes of river in Southeast Tibet are generally large and distributed exponentially. The channel slope of the measuring points for approximately 80% is greater than 10% and for more than 50% of the measured points is greater than 2%. There are 3 measurement points where the channel slope is greater than 30% (48%, 35% and 32%). The largest two channel slopes are located on the Ganongqu tributary at the Zhamo Highway and at the Yanatongqu near Guoluo village, Basu county, Changdu. The point where the channel slope is 32% is located at Renatongqu river near Guoluo village, Basu county, Changdu. These three measuring points belong to rivers that flow into the valley from steep hillsides at an angle close to the vertical valley. In southeastern Tibet, rivers flow fast, and the slopes are steep. After heavy rainfall, the confluence time of floods is short, so flash floods with short occurrence times and high intensities often form, resulting in large economic losses and casualties of human and livestock[19].

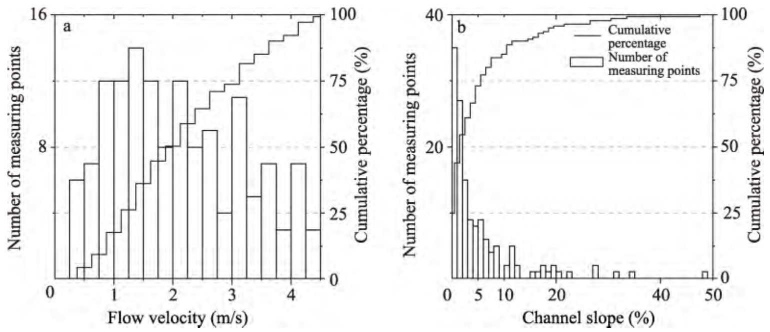

Figure 5 Statistical distribution of measured flow velocity (a) and channel slope (b).

4.2 The Relationship between Stream Flow Velocity and Strahler Order

Based on the collected data, the velocity of rivers in the southeastern Qinghai-Tibet Plateau is exponentially related to the Strahler order (Figure 6). Using the traditional Strahler river characteristic analysis method[20], the flow velocity and characteristic values were classified according to the Strahler order. Although the velocity of the same order river varies greatly, in general, the average velocity (v) of the river increases exponentially with the increase in Strahler order (ω). The fitted exponential function is:

$$v = 1.116e^{0.158(\omega-1)} \tag{1}$$

At a significance level of $p < 0.001$, the Strahler order of the river explained 91% of the variance in the average river velocity (R^2 = 0.911). The average velocity of the first order rivers measured in the southeastern Qinghai-Tibet Plateau is 1.10 m/s, and the fitted value based on Equation (1) is 1.12 m/s. Although there is some fitting error in the velocity- Strahler order relationship of the river, the relationship can be used for the simple calculation of velocity in areas with scarce data in the southeastern Qinghai-Tibet Plateau.

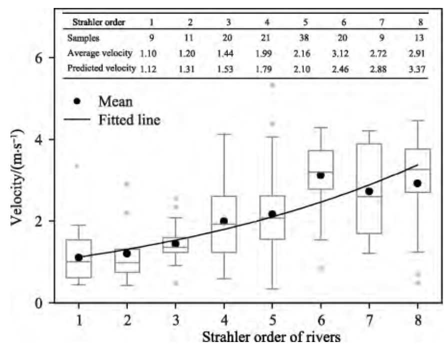

Figure 6 The relationship between river velocity and Strahler order in the southeastern Qinghai-Tibet Plateau

4.3 Pattern of Flow Velocity from the River Mouth to Its Source

Taking the Sangqu, Lengqu and Puqu rivers as examples, Figure 7 shows the changes in the stream flow velocity, river width and slope of the three rivers (Sangqu, Lengqu and Puqu rivers) from the river mouth to the source of the river. From the simple linear fit between flow velocity and the distance from the river mouth to the source, the slopes of all fitted lines are negative (–0.009, –0.017 and –0.044, respectively, excluding singular values). The significance levels of the fit relationship were < 0.01, < 0.01 and < 0.1 (excluding singular values). The flow velocity of the three rivers gradually decreases from the river mouth to the source. This result is inconsistent with the general impression that rivers in mountainous areas have relatively steep slopes, and so the flow velocity is greater than that of rivers in relatively flat areas downstream.

According to the Manning equation, the channel slope and hydraulic radius (when the river width is much greater than the water depth, the hydraulic radius is approximately equal to the water depth) are the main factors influencing stream flow velocity[21]. Generally, the slope upstream is greater, but the runoff (or water depth) downstream increases with the increase in catchment area or the number of confluence tributaries. Therefore, the change in velocity from the source area to the river mouth along the same river is the combined effect of slope and flow.

The above data and analysis show that for the Sangqu, Lengqu and Puqu rivers, the closer the distance to the river mouth, the larger the catchment area and/or the greater the number of tributaries. Although the stream flow velocity decreases from the river mouth to the source, the overall trend may show small fluctuations due to local river slope and river width changes. For example, the Puqu river shows the stream flow velocity that differs from the overall trend at the maximum value of river width and the maximum value of channel slope (Figure 7). When these two singular points are included, the slope of the general curve fitting equation is –0.004, and the statistical test is not significant. When they are not included, the downward trend of the velocity tracing becomes 0.044 m/s per kilometer and passes the statistical significance test at the level of p = 0.1. It shows that there are fewer tributaries on both sides of the Puqu river, and the increase in river water volume is not as great as that in the Sangqu river and Lengqu river.

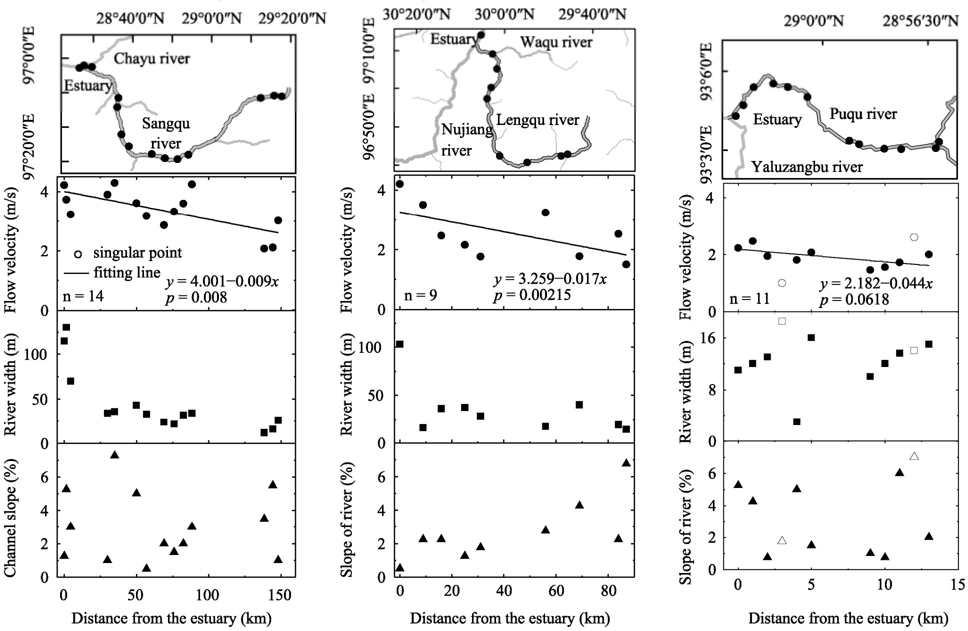

Figure 7 Changes in velocity, width and slope of the Sangqu river, Lengqu river and Puqu river from the river mouths to their sources

5 Discussion and Conclusion

The dataset was developed through field measurements based on a handheld radar current meter (RD-60) and outdoor rangefinders. By analyzing the statistical distribution characteristics of the data, the relationship between the velocity and the Strahler order of river, and the pattern of flow velocity from the river mouth to the channel head, the following conclusions are drawn: compared with plain areas, the flow velocity of the Qinghai-Tibet Plateau is generally higher; as a whole, the higher the Strahler order, the faster the river flows; in some rivers on the Qinghai-Tibet Plateau, the closer the distance to the river mouth, the higher the stream flow velocity, and the increase of stream flow velocity mainly comes from the increase in runoff.

Author Contributions

Chen, B., Pu, H. C., and Xiao, Y. designed the survey and compiled the dataset. Xiao, Y., Pu, H. C., and Chen, B. contributed to the data collection, processing and analysis. Pu, H. C. and Chen, B. wrote the paper. Liu, L.Y., Shi, P. J., Yan, P., Zhang, G. M., and Liu, J. F. discussed the data collection plan and revised the manuscript.

Acknowledgements

We thank Professor Yang, W. T. for helpful discussion and Ouzhu, P. J. and others for their patient and kind help with data collection.

Conflicts of Interest

The authors declare no conflicts of interest.

References

[1] Fu, M. N. The response of climate change in the Qinghai Tibet Plateau to the challenge of disaster prevention and reduction in China [J]. *Disaster Reduction in China*, 2021(7): 46–49.

[2] Wang, X. J., Cheng, S. M. Analysis of major climate characteristics in Tibet [J]. *Plateau and Mountain Meteorology Research*, 2009, 29(4): 81–84.

[3] Ma, W. D., Liu, F. G., Zhou, Q., *et al*. Characteristics of extreme precipitation over the Qinghai-Tibet Plateau from 1961 to 2017 [J]. *Journal of Natural Resources*, 2020, 35(12): 3039–3050.

[4] Qi, W., Liu, S. H., Zhou, L. Regional differentiation of population in Tibetan Plateau: insight from the “Hu Line” [J]. *Acta Geographica Sinica*, 2020, 75(2): 255–267.

[5] Wu, J. L., Cheng, Z. S., Geng, X. Y. Formation of dam from debris flow in the Southeast Tibet [J]. *Mountain Research*, 2005(4): 4399–4405.

[6] Li, L., Chen, X. G., Wang, Z. Y, *et al*. Climate change and its regional differences over the Tibetan Plateau [J]. *Climate Change Research*, 2010, 6(3): 181–186.

[7] Xu, L. J., Hu, Z. Y., Zhao, Y. N., *et al*. Climate change characteristics in Qinghai-Tibetan Plateau during 1961 2010 [J]. *Plateau Meteorology*, 2019, 38(5): 911–919.

[8] Gong, T. L., Wang, X. J., Xie, Y. H., *et al*. The spatial distribution characteristics of Tibet hydrological monitoring network [J]. *Journal of China Hydrology*, 2004(6): 41–43.

[9] Lan, C., Zhang, Y. X., Zhu, F. X., *et al*. Characteristics and changes of streamflow on the Tibetan Plateau: a review [J]. *Journal of Hydrology*: *Regional Studies*, 2014, 2: 49–68.

[10] Pu, H. C., Chen, B., Xiao, Y., *et al*. Pre-flood environment field survey dataset in Southeastern Tibet of China (2021) [J/DB/OL]. *Digital Journal of Global Change Data Repository*, 2021. https://doi.org/10.3974/geodb.2021.10.03.V1. https://cstr.escience.org.cn/CSTR:20146.11.2021.10.03.V1.

[11] GCdataPR Editorial Office. GCdataPR data sharing policy [OL]. https://doi.org/10.3974/dp.policy.2014.05 (Updated 2017).

[12] Ma, W. D. Characteristics of extreme precipitation in Qinghai-Tibet Plateau and estimation of critical rainfall for flood disasters [D]. Xining: Qinghai Normal university, 2019.

[13] Ruan, B. Q., Wang, H. Resource conditions and discussion on possible quantity of water transfered from the southwest to north China [J]. *Journal of Tsinghua University* (*Science and Technology*), 2000(S1): 101–106.

[14] Liu, G. W. Hydrometeorological characteristics of the Tibet Plateau [J]. *Journal of Hydraulic Engineering*, 1992(5): 1–8.

[15] Zong, X. G., Wang, J., Xu, W. G. The Application of bridge survey technology in the tour survey in the plain area of North Shandong province [J]. *Journal of China Hydrology*, 2004, 24(3): 46–50.

[16] Zuo, J., Deng, S., Zhang, H. X., *et al*. Representative study of surface velocity at Baihe Hydrological Station [J]. *Journal of China Hydrology*, 2021, 41(3): 19–24.

[17] Strahler, A. N. Quantitative analysis of watershed geomorphology [J]. Eos, *Transactions American Geophysical Union*, 1957, 38(6): 913–920.

[18] Zhang, D. L. The temporal and spatial variations of water resources over the Tibetan Plateau [D]. Lanzhou: Lanzhou university, 2013.

[19] Gao, M. F., Qiu, J. J. Characteristics and distribution law of major natural disasters in Tibetan Plateau [J]. *Journal of Arid Land Resources and Environment*, 2011, 25(8): 101–106.

[20] Downing, J. A., Cole, J. J., Duarte, C. M., *et al*. Global abundance and size distribution of streams and rivers [J]. *Inland Waters*, 2012, 2(4): 229–236.

[21] Jain, S. C. Open-channel Flow [M]. Hoboken: John Wiley & Sons, 2000.